Impacts of Anthropogenic Aerosol Emissions on the East Asian Winter Monsoon

Shenglong Zhang (zhangsl21@mails.tsinghua.edu.cn) and Jonathon S. Wright
Department of Earth System Science, Tsinghua University

清华大学地球系统科学系
Department of Earth System Science, Tsinghua University

Key points

- The Community Integrated Earth System Model (CIESM) captures the East Asian Winter Monsoon (EAWM) mean state well
- Anthropogenic aerosols strengthen the EAWM, making East Asian land areas **colder, drier, and snowier**
- These aerosol effects are comparable to **half the difference between strong and weak EAWM episodes** in the control simulation
- **Aerosol effects on both radiative and non-radiative heating** contribute to intensifying the PV intrusion and strengthening the EAWM

Mean state of EAWM

- The Tsinghua University Community Integrated Earth System Model (CIESM) **captures the mean state East Asian Winter Monsoon (EAWM) well** when compared with ERA5
- A stronger southward intrusion of positive potential vorticity (PV) anomalies is associated with negative surface air temperature anomalies over mid-latitude East Asia
- Anthropogenic aerosol emissions **stabilize the troposphere** and **strengthen the intensity of the EAWM** relative to the control (BASE) case.

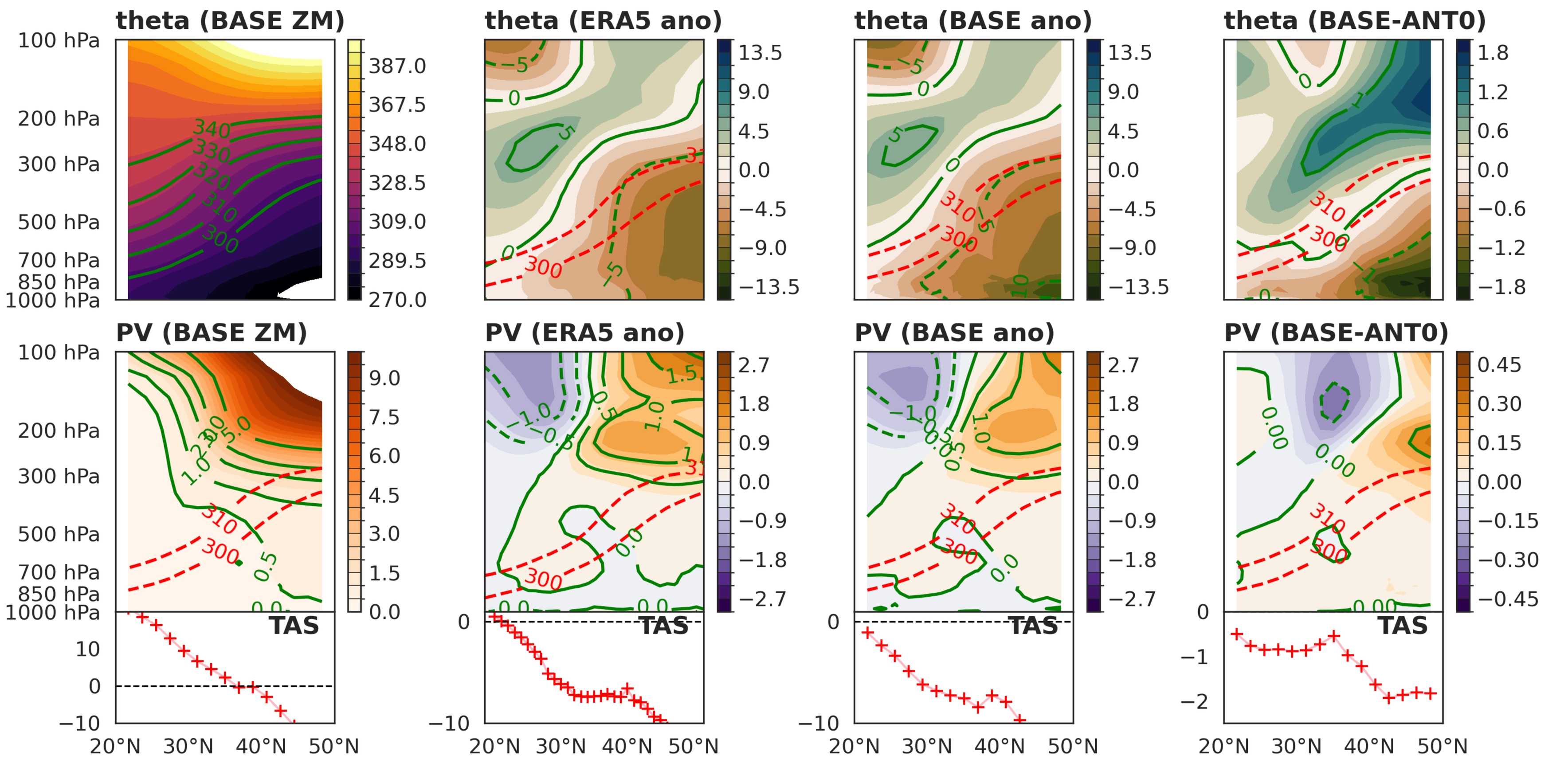

Figure 1. East Asian zonal mean potential temperature (θ), potential vorticity (PV), and surface air temperature (TAS) from BASE (left); differences between the East Asian and global zonal means from ERA5 (left center) and BASE (right center); and differences between BASE and ANT0 (right) for November–March of 1999–2018

Aerosol effects on EAWM

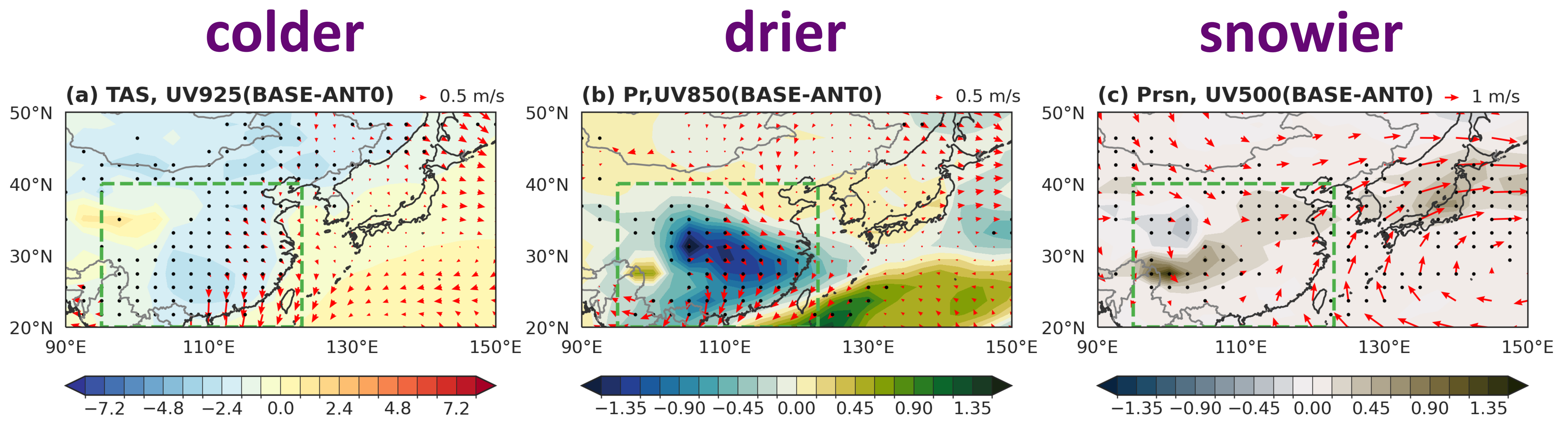

Figure 2. Differences in mean surface air temperature (TAS, K), precipitation (Pr, mm·d^{-1}), and snowfall (Prsn, mm·d^{-1}) during November–March of 1999–2018 between the BASE and ANT0 scenarios

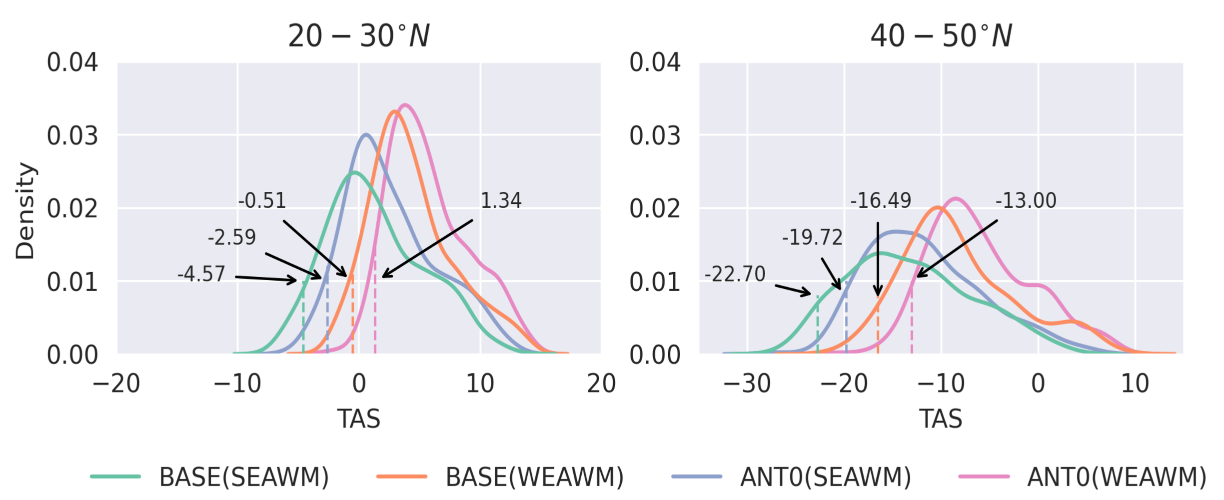

- The coldest 10% of days during strong and weak EAWM periods are **~2°C colder in the south** and **~3°C colder in the north** in BASE relative to ANT0
- These changes are **about 50% of the difference between strong and weak EAWM** periods

Figure 3. Surface air temperature (TAS, K) distributions for strong and weak EAWM days over southern (left) and northern (right) East Asia during November–March of 1999–2018 under the BASE and ANT0 scenarios

Thermodynamic mechanisms of anthropogenic aerosol effects on EAWM

- A strong EAWM is usually associated with an amplified Siberian High and Aleutian Low at the surface and an accelerated East Asian jet in the upper troposphere
- Anthropogenic aerosol effects **intensify the zonal pressure dipole** and **shift the East Asian jet and storm track northward**

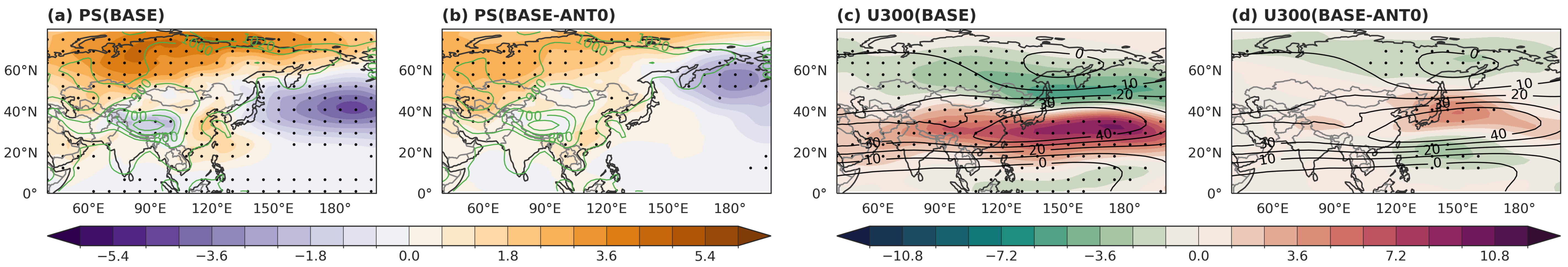

Figure 4. Anomalies in surface pressure (PS; a) and 300 hPa zonal wind (U300; c) from the BASE scenario regressed onto the detrended and standardized PV-based EAWM index time series, and differences of PS (b) and U300 (d) between the BASE and ANT0 scenarios for November–March of 1999–2018

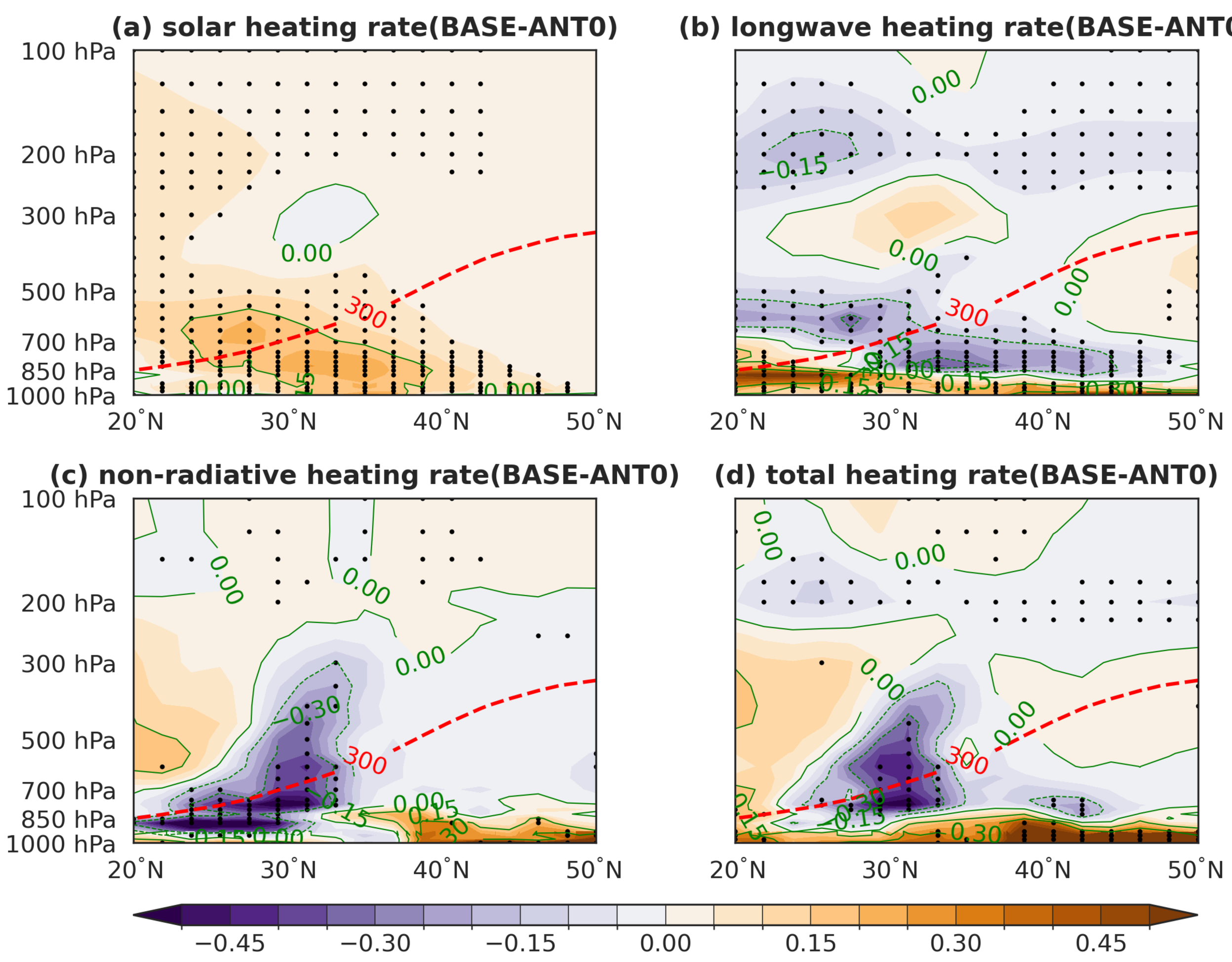

Figure 5. latitude-pressure section of the differences in solar radiative heating rate, longwave radiative heating rate, non-radiative heating rate, and total heating rate ($\frac{\partial\theta}{\partial t}$, K·d^{-1}) between BASE and ANT0 scenarios

- Anthropogenic aerosols increase shortwave absorption, **warming the lower–middle troposphere** (direct effect)
- Anthropogenic aerosols **increase longwave heating near the surface and longwave cooling in the lower troposphere**
- Differences in non-radiative heating indicate **reduced latent heating over southern East Asia (less precipitation)** and widespread changes in boundary layer turbulence
- Anthropogenic aerosols warm the atmosphere over the Tibetan Plateau

$$\frac{dPV}{dt} = PV\cdot\boxed{\frac{\partial}{\partial\theta}\left(\frac{\partial\theta}{\partial t}\right)} - \frac{\partial\theta}{\partial t}\cdot\frac{\partial PV}{\partial\theta},\ PV = -g(\zeta+f)\frac{\partial\theta}{\partial p}$$

- Aerosol **radiative and non-radiative effects both contribute to strengthening the winter monsoon**
- Increased precipitation over the western North Pacific is linked to decreased vertical gradient of longwave radiative heating

Figure 6. Differences in the vertical gradient of solar heating, longwave heating, non-radiative heating, and total heating ($\frac{\partial\dot{\theta}}{\partial p}$, K·d^{-1}·K^{-1}) across the 300K isentropic level between the BASE and ANT0 scenarios. Values are masked where the 300K isentropic surface intersects the atmospheric boundary layer

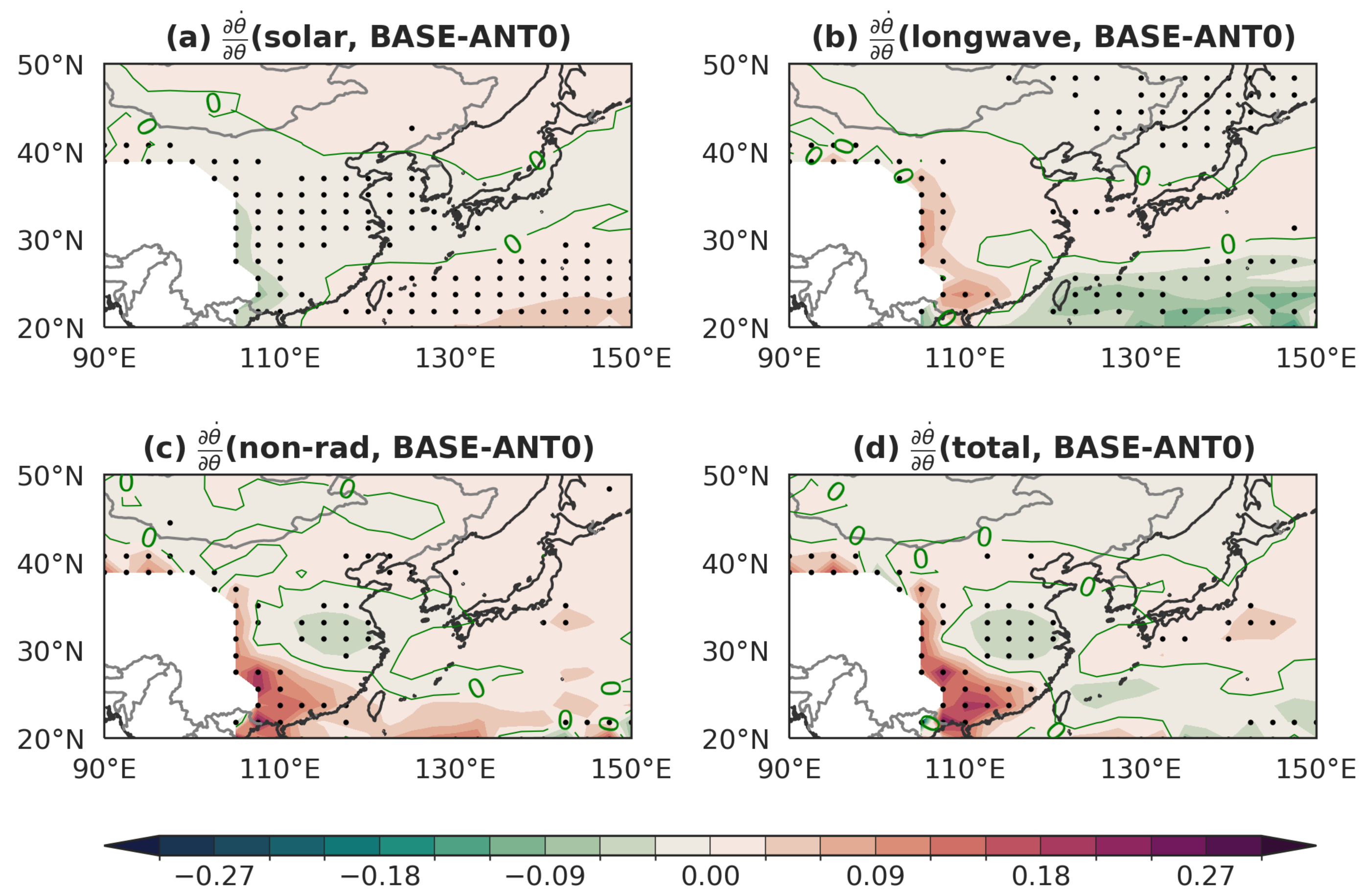

References

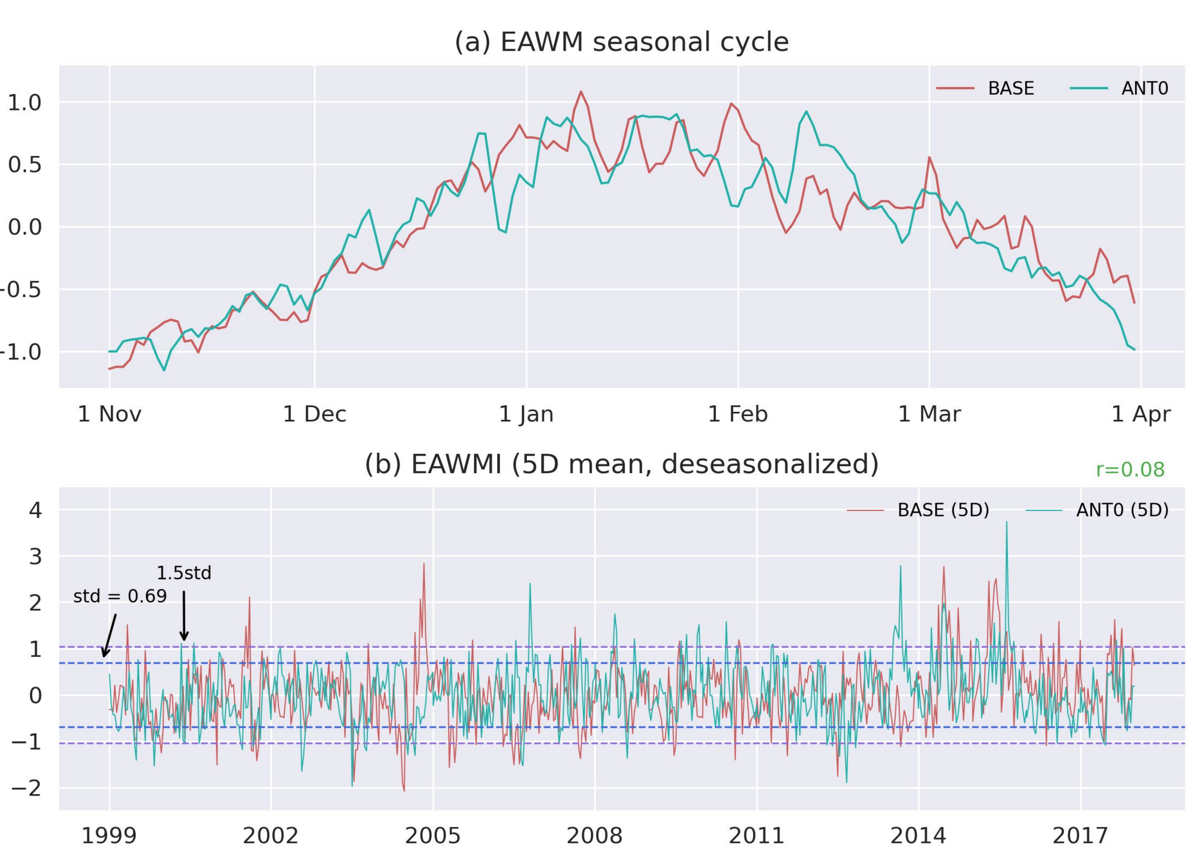

Figure 7. EAWM seasonal cycle and rolling 5-day mean deseasonalized EAWM index for November–March of 1999–2018 from BASE and ANT0

The PV-based EAWM index used in this work captures relationships between the EAWM and the Siberian high and Arctic Oscillation, tracing the roots of cold air intrusions to high altitudes in the Arctic. To limit noise due to frictional effects in the boundary layer, we define a modified PV-based EAWM index as follows.

$$\mathrm{PV}^m_{300K} = \mathrm{PV}_{300K}(P_{300K} > P_{\mathrm{ABL}})$$

$$I^m_{EAWM} = \overline{\mathrm{PV}^m_{300K}(90-150°\mathrm{E}, 20-50°\mathrm{N})} - \overline{\mathrm{PV}^m_{300K}(0-360°\mathrm{E}, 20-50°\mathrm{N})}$$

A more detailed introduction to the PV-based EAWM index is available via the QR code:

The Tsinghua University Community Integrated Earth System Model (CIESM) includes many new developments and changes that alleviate some persistent climate model biases. More details are available via the QR code at right.

The results presented here are based on model simulations conducted for the AeroCom Phase III ACAM model experiments targeting climate impacts of aerosol emissions. More information is available via the QR code at right.